Al-Mg ISOTOPE STUDY OF ALLENDE 5241. A. G. Kerekgyarto[1], C. R. Jeffcoat[1], T. J. Lapen[1], R. Andreasen[2], M. Righter[1], D. K. Ross[3,4], J. I. Simon[4], [1]Department of Earth and Atmospheric Sciences, University of Houston, Houston, Tx 77204 (agkerekgyarto@uh.edu), [2]Dept. of Geoscience, Aarhus University, Denmark. [3]Jacobs Tech, NASA-JSC, Houston, Tx 77058. [4]Center for Isotope Cosmochemistry and Geochronology, ARES NASA-JSC, Houston, Tx 77058.

Introduction: The defining characteristic of type B1 CAIs is a large (.5- 3mm) concentric melilite mantle [1]. In [2] we presented two isochrons from separate traverses across the melilite mantle of Allende EK 459-5-1. The primary petrographic differences between the traverses was the preservation of strong oscillatory zoning. The traverse that crossed the distinctive oscillatory zone produced a pristine internal isochron, while the other that did not have a strongly preserved oscillatory zone produced a disturbed isochron indicated by more scatter (higher MSWD) and a positive δ^{26}Mg* intercept. The implication simply being that the oscillatory zone may represent varying conditions during the mantle formation event. We targeted a similar texture in Allende 5241 using the same methodology in an attempt to achieve similar results.

Allende 5241 (or USNM 5241, or NMNH 5241) is a type B1 CAI fragment measuring ~12 by ~8 mm and is currently on loan from the Smithsonian Institution. This inclusion has been the focus of several studies [3, 4, 5,6, 7, 8]. The inclusion shows many of the same physical features as EK 459-5-1: 1) Spinel-free interiors (SFIs), 2) concentric mantle textures with the inner most being oscillatory zoned and aligned with small fassaite grains, 3) fassaite 'blebs' with correlated higher Åk# in outer mantle, 4) large chaotic and concentric zoned interior fassaite, 5) similar secondary phases derived from reactions between melilite and anorthite, 6) numerous fremdlinge, and 7) a small WL rim. These may point to a similar formation and evolution history of the two CAIs. Literature on this object strongly focuses on the formation of the CAI, its mantle, and the SFI. [8], through Al-Mg attempted to correlate the petrographic zones of the inclusion with $^{26}Al/^{27}Al_0$. The inclusion, EGG-6 [6] is reported to have a similar oscillatory zoning as Allende 5241, and EK 459-5-1. If the oscillatory zoning of the melilite mantle is primary, it would be a potentially ideal place to look for pristine Al-Mg systematics.

Methodology: 5241 was characterized using a JEOL JSM-7600F SEM and a JEOL 8530F HyperProbe EPMA at JSC. *In-Situ* Al-Mg isotope studies were done on a Nu Plasma II MC-ICP-MS with an Analyte 193nm excimer laser system. The laser was operated with a spot size of 50 µm, 10 Hz rep rate and a fluence of 2.99 J/cm^2. ^{24}Mg, ^{25}Mg, ^{26}Mg, and ^{27}Al were all measured simultaneously using faraday collectors. Natural gehlenite standards were used to correct

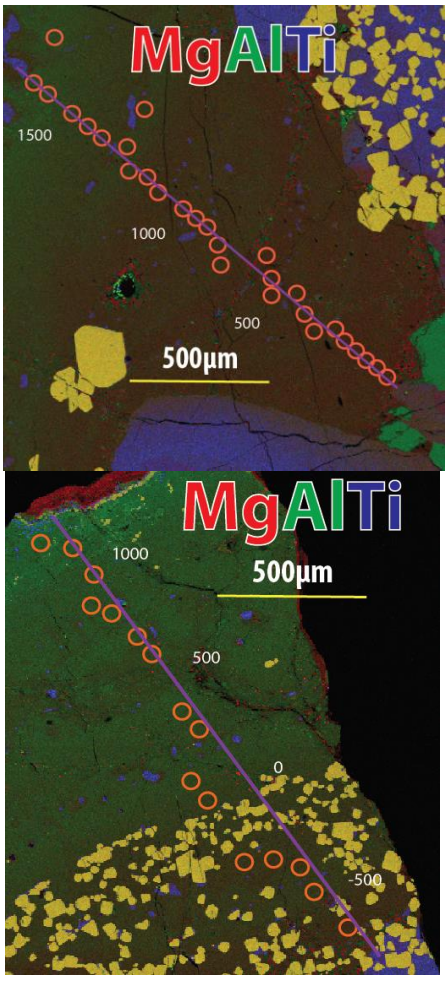

Figure 1: RGB (Mg-Al-Ti) map of Allende 5241. 50 µm spot locations for radiogenic, and stable Mg data shown in orange. EMPA line traverse shown in purple. Top: Oscillatory zone through 'SFI' in core-mantle boundary. Bottom: Full melilite mantle line

for instrumental mass bias and elemental fractionation. $^{27}Al/^{24}Mg$ values were compared to electron microprobe data to verify the accuracy. The data are reported in δ notation relative to DSM3 [9]. A β-value of 0.5128 was used for calculating the radiogenic Mg (δ^{26}Mg*) [10]. Ca^{48++} was corrected via a calibration curve using terrestrial phases of varying Ca/Mg ratios up to that of anorthite (Ca/Mg = 198).

Two linescans across the melilite mantle were performed, one across the oscillatory zone. Another line scane was performed, where the oscillatory zoning is not as prominent (melilite mantle). Laser spot locations and EPMA line scans can be seen in figure 1. Interior

anorthite from both the SFIs and the spinel rich areas were also collected.

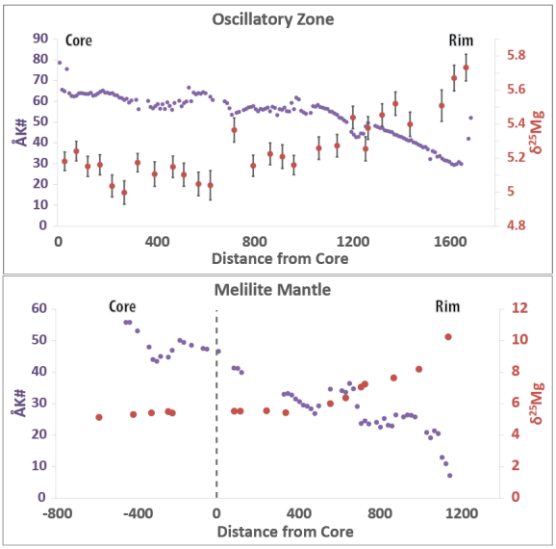

Figure 2: Åk# and δ^{25}Mg plotted vs distance from the core-mantle boundary. Error bars are 2σ, and are smaller than the data points in some cases (bottom). Notice scale differences between δ^{25}Mg profiles, as the oscillatory traverse does not continue across the entire mantle.

Results: Al-Mg regressions of the melilite mantle data produced a $(^{26}Al/^{27}Al)_0$ of 3.33 (±0.14) x 10^{-5}, and $\delta^{26}Mg^*_0$: 0.06 ± 0.05, in perfect agreement [8]. Tying these data to anorthite in the core produced a $(^{26}Al/^{27}Al)_0$ of 4.73 (±0.10) x 10^{-5}, and $\delta^{26}Mg^*_0$: -0.39 ± 0.53. These anorthite data are from multiple SFIs, spinel rich areas and near the core-mantle boundary and might have succumbed to local equilibria, but overall this again is in perfect alignment with the interior isochrons found in [8]. Stable δ^{25}Mg profiles are shown in figure 2. The oscillatory zone shows an over all increase of ~.8 permil from core to the end of the oscillatory zone (about half way through the mantle). The melilite mantle line scan shows a more complete view of the stable isotope profile through the mantle increasing from ~5 to ~10 from core to rim.

Discussion/Conclusion: Allende 5241 and EK-459-5-1 show remarkably similar petrographic features. The isotope profiles, though, are considerably different. [11] shows the δ^{25}Mg profile decreasing by ~1 permil from core to rim (~8-7), while 5241 increases from core to rim (5 to 10 permil). EK 459-5-1 has a melilite mantle which formed, or at least locked-in ^{26}Al, considerably earlier than 5241. While anorthite shows the most radiogenic regression in 5241, in EK 459-5-1 the anorthite is the least radiogenic for its $^{27}Al/^{24}Mg$.

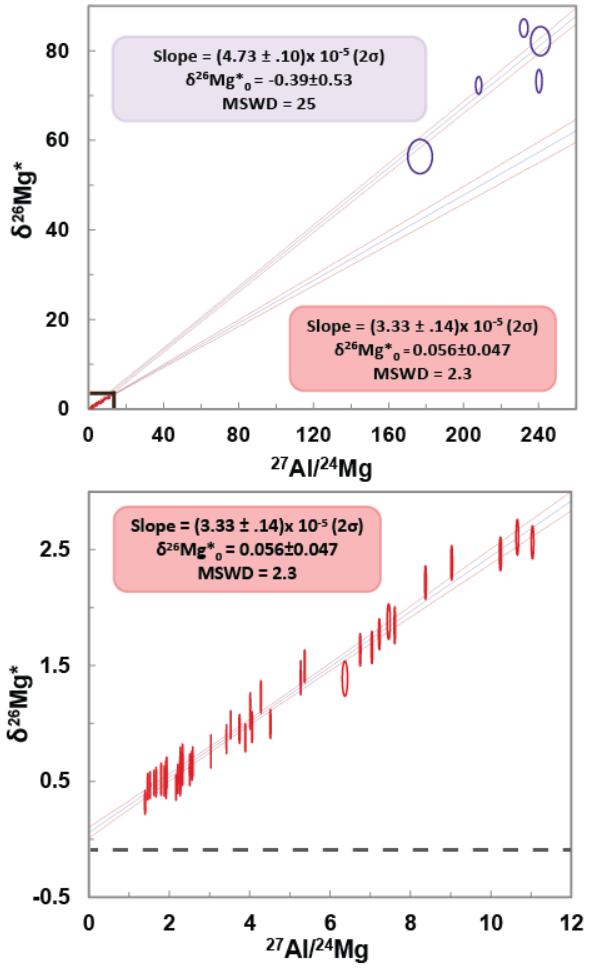

Figure 3: Top: All mantle data points including anorthite and not including anorthite. $(^{26}Al/^{27}Al)_0$ of 4.73 (±0.10) x 10^{-5}, $\delta^{26}Mg^*_0$: -0.39 ± 0.53, and $(^{26}Al/^{27}Al)_0$ of 3.33 (±0.14) x 10^{-5}, $\delta^{26}Mg^*_0$: 0.06 ± 0.05 respectively. Bottom: Isochron of just the melilite mantle data points, shown in bottom-left corner of (top).

References: [1] Wark D. A. and Lovering J. F. (1982) *GCA, 46*, 2581-2594. [2] Kerekgyarto A. G. et al. (2015) *LPS XLV1*, 1832. [3] El Goresy A. et al. (1985) *GCA, 47*, 1635-1650. [4] MacPherson G. J. et al. (1989) *GCA*, 53, 2413-2427. [5] Meeker G. P. (1995) *MAPS, 30*, 71-84. [6] Meeker G. P. (1995) *LPS XXVI*, 947-948. [7] Davis A. M. et al. (1998) *LPS XXIX*, 1948. [8] Hsu W. et al. (2000) *EPSL* 182, 15-29. [9] Galy A. et al. (2003) *JAAS* 18, 1352-1356 [10] Davis A. M. et al. (2015) *GCA* 158, 245- 261. [11] Kerekgyarto A. G. et al. (2014) *LPS XLV*, 2874